Journal of Applied Electrochemistry (2006) 36:375–383
DOI 10.1007/s10800-005-9083-x

Evaluation of the corrosion behavior of galvannealed steel in chloride aqueous solution and in tropical marine environment

PAULO S. G. DA SILVA[1], ALBERTO N. C. COSTA[2], OSCAR R. MATTOS[3], ADRIANA N. CORREIA[1] and P. DE LIMA-NETO[1,*]
[1]*Departamento de Química Analítica e Físico-Química, Universidade Federal do Ceará, C.P. 6035, 60455-970, Fortaleza, CE, Brazil*
[2]*Gerência de Pesquisa e Desenvolvimento, CSN, Volta Redonda, RJ, Brazil*
[3]*Laboratório de Corrosão Prof. Manoel de Castro, PEMM/COOPE/UFRJ, Rio de Janeiro, RJ, Brazil*
*(*author for correspondence: e-mail: pln@ufc.br)*

Received 12 January 2005; accepted in revised form 28 September 2005

Key words: corrosion, electrochemistry, galvanized steel, galvannealed steel, tropical marine environment

Abstract

An investigation was made into the corrosion behavior of commercial galvannealed steel in 10^{-2} mol dm^{-3} NaCl aqueous solutions and in a tropical marine environment, using scanning electron microscopy (SEM), galvanostatic electrochemical stripping (GES), potentiodynamic linear polarization (PLP), and electrochemical impedance spectroscopy (EIS) techniques and open circuit measurements (E_{oc}). For purposes of comparison, a commercial galvanized steel was also subjected to similar corrosion tests. GES and SEM techniques allowed for the identification of ζ, δ and Γ intermetallic phases and revealed cracks in the galvannealed steel. The PLP, EIS and E_{oc} results indicated that the galvannealed coating was more corrosion resistant than galvanized coating in an aqueous medium, but that their corrosion behaviors were similar in the marine environment. The corrosion behavior of the galvannealed steel was affected by the evolution of the cracking process in the Zn–Fe layer due to the dissolution of zinc-rich phases, while the galvanized steel displayed generalized corrosion in the aqueous medium and localized corrosion in the marine environment.

1. Introduction

It is well known that galvannealed (Zn–Fe) coatings possess higher corrosion resistance and better painting and welding properties than galvanized (Zn) coatings. Galvannealed coatings, which are produced by rapid annealing of galvanized steel at temperatures ranging from 490 °C to 540 °C, consist of several zinc–iron intermetallic phases: the ζ, the δ and the Γ phases [1–3]. Due to its superior properties, galvannealed steel has been increasingly used in the automotive industry and interest in understanding its corrosion behavior has grown [4–12].

Although galvannealed steel is applied on an industrial scale, reports in the literature regarding its corrosion behavior are mainly based on laboratory ageing tests. Samples of galvanized and galvannealed coatings in alkaline mediums have revealed that the products of corrosion are modified by the chloride content in solution. Moreover, the passivation process for both zinc-rich ξ and δ phases is diffusion-controlled over the range of pH 9–14 [6]. The electrochemical stripping technique has been used to characterize the Zn–Fe intermetallic phases present in galvannealed coatings [7–11] and in synthesized alloys [9]. Fabri-Miranda et al. [12], who studied the corrosion of galvannealed steel exposed to an industrial environment for a year, concluded that the corrosion process was associated with the presence of depressions in the external coating surface related to the presence of ξ and δ Zn–Fe intermetallic phases. However, the literature offers little data about the corrosion behavior of these coatings in natural environments, particularly in tropical marine environments.

Therefore, this study investigated the corrosion behavior of unpainted galvannealed coatings undergoing long-term exposure to both aerated NaCl aqueous solutions and to Brazil's northeastern tropical marine environment, hoping to shed light on the corrosion mechanism of Zn–Fe coating. For purposes of comparison a galvanized coating was also studied under the same conditions. Environmental corrosion tests were conducted in Fortaleza, a tourist and industrial city located on Brazil's northeastern coast. Fortaleza's environmental conditions are extremely aggressive to metals and alloys, with an average annual ambient temperature of about 30 °C, a summer-like climate throughout the year, and constant winds blowing inland off the ocean.

2. Experimental details

2.1. *Material*

Samples of galvannealed and galvanized steel sheets were supplied by Companhia Siderúrgica Nacional (CSN), Volta Redonda, RJ, Brazil. The iron content in the galvannealed coating, which was determined by localized EDAX analyses at seven different points of the Zn–Fe surface, presented an average value of 12.5 at% (±1.1 at%).

2.2. *Physical characterization*

The microstructure of the as-received and tested samples was analyzed by scanning electron microscopy (SEM) using a Philips XL-30 microscope. Samples for SEM cross-section analysis were previously embedded in epoxy resin, polished with SiC sandpaper up to 600 grit, then with alumina ($\phi = 0.3$ μm) or diamond paste ($\phi = 0.3$ μm), and finally subjected to chemical etching in a solution of 5% HNO_3 in ethanol. Chemical analyses of the samples before and after the corrosion tests were conducted using a Link Analytical QX-2000 energy dispersive X-ray analyzer (EDAX) attached to the SEM apparatus.

2.3. *Corrosion tests*

The marine environment corrosion tests involved the 3-year exposure of galvannealed and galvanized steel samples, according to the ASTM G-50 Standard [13]. The deterioration of exposed samples was assessed using a method established in our group [12, 14]. This method consists of periodically removing samples from the corrosive environment to which they are exposed and subjecting them to laboratory analyses by electrochemical impedance spectroscopy (EIS) at open circuit potential (E_{oc}), after which they are returned to the corrosive environment. The electrolyte was a 10^{-2} mol dm^{-3} NaCl aqueous solution. The samples were analyzed in the conditions of exposure, with the products of corrosion on their surfaces. This is a non-destructive test that does not influence the subsequent corrosion behavior. All the corrosion tests performed in the laboratory were conducted at room temperature (25 ± 1 °C).

Mass loss tests were performed by immersing the samples in a NaCl solution for 20 days, followed by chemical attack in a 10% glycine solution for 10 min, according to the method proposed by Beccaria [15]. The electrochemical laboratory tests involved the following electrochemical techniques: galvanostatic electrochemical stripping (GES), potentiodynamic linear polarization (PLP), EIS and E_{oc} measurements. All the electrochemical experiments were conducted on duplicate samples. The electrochemical cell consisted of a PVC tube glued to the surface, exposing an area of approximately 11 cm^2 during the GES and PLP tests, while a cell with a Teflon sample holder exposed about 55 cm^2 in the EIS measurements. Pt foil and saturated calomel (SCE) were used, respectively, as auxiliary and reference electrodes.

The GES experiments were galvanostatically controlled at 2 mA cm^{-2} using 3.4 mol dm^{-3} NaCl and 0.6 mol dm^{-3} $ZnSO_4$ as electrolyte. The evolution of the EIS diagrams with immersion time (long-term laboratory tests) for the samples immersed in the 10^{-2} mol dm^{-3} NaCl aqueous solution was assessed at E_{oc}. The EIS experiments were conducted in a frequency range of 5 mHz to 10 kHz and an amplitude perturbation of 5 mV. All the working solutions were prepared with Milli-Q water and analytical grade chemical reagents. A potentiostat/galvanostat AUTOLAB PGSTAT 30 linked to a PC microcomputer and controlled by GPES and FRA software was used to acquire and analyze the electrochemical data.

3. Results and discussion

3.1. *Electrochemical and morphological characterizations*

Figure 1 shows the potential-time curves obtained from galvanostatic stripping of the galvannealed and galvanized coatings. The galvannealed coating consistently showed more positive potential values than did the galvanized coating due to its content of iron, an element with a nobler thermodynamic standard electrochemical potential. While the curve corresponding to the galvanized coating presented a single and well defined plateau at 1.0 V, the curve for the galvannealed coating presented three potential plateaus, two of them well defined at −0.91 V and −0.75 V and a short broad one at −0.82 V. These results are in close agreement with those previously reported [5–11]. Based on these studies, the plateau observed at −1.0 V can be attributed to the η phase, corresponding to the Zn layers, while those observed at −0.91 V, −0.82 V and −0.75 V can be ascribed, respectively, to the ξ, δ, and Γ Zn–Fe intermetallic phases. The short potential plateau

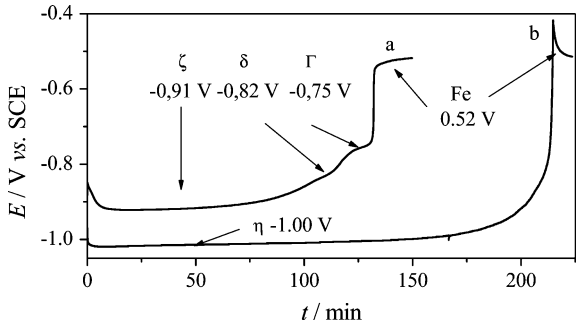

Fig. 1. Potential-time curves obtained from galvanostatic stripping of the galvannealed (a) and galvanized (b) coatings in 3.4 mol dm^{-3} NaCl and 0.6 mol dm^{-3} $ZnSO_4$ at 2 mA cm^{-2} and room temperature.

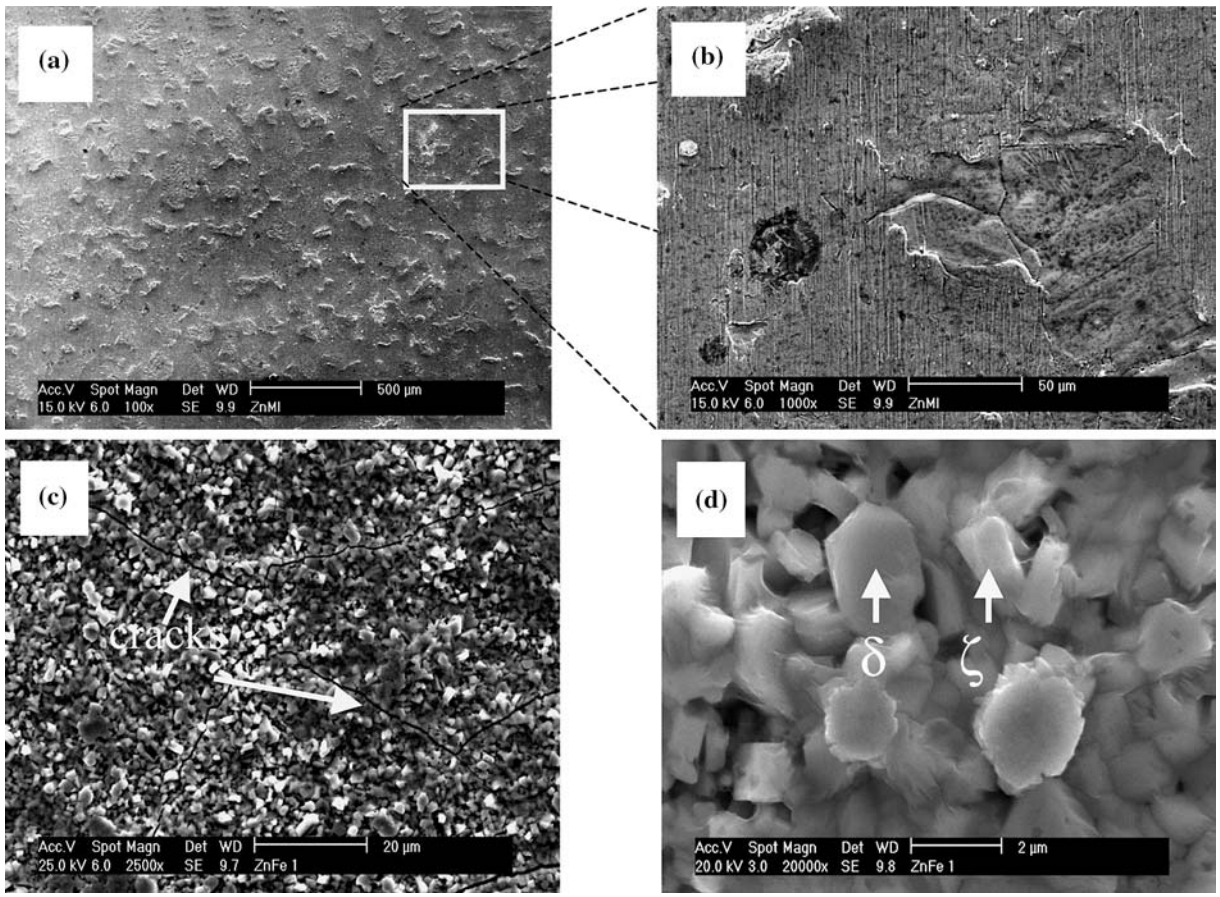

Fig. 2. SEM micrographs showing the surface morphology of the as-received galvanized (a, b) and galvannealed (c, d) coatings.

observed at −0.52 V corresponds to the dissolution of Fe from the steel substrate.

Figure 2 shows a SEM image of the surface morphology of as-received galvanized and galvannealed steels. The galvanized steel displayed a homogeneous surface devoid of surface cracks (Figure 2a). A detailed SEM analysis (Figure 2b) revealed a few superficial defects which probably resulted from the industrial hot dip galvanizing process [1]. On the other hand, the as-received galvannealed steel surface was granular, with hairline cracks (Figure 2c). A detailed SEM analysis (Figure 2d) enabled us to identify hexagonal and monoclinic crystals associated, respectively, with δ ($FeZn_7$) and ξ ($FeZn_{13}$) intermetallic phases [7, 12]. The presence of hairline cracks is typical of other Zn–alloy electrocoatings, such as Zn–Ni electrodeposits [14], and may be related to the internal stress of the coating that develops as the coating is formed. Cracking in Zn–Fe coatings is caused by heat-treating galvanized steel [12]. The SEM micrograph of the as-received galvannealed steel does not show depressions on the surface coating, such as those observed by Fabri-Miranda et al. in galvannealed coating samples produced on an industrial continuous galvanizing line [12].

Figures 3 and 4 show the metallographic cross-section of the as-received and tested galvanized and galvannealed samples. The micrograph in Figure 3a reveals a homogeneous and compact as-received galvanized layer. The measurements taken at different points of the coating indicated that the average thickness of the Zn layer was 15.36 ± 0.5 µm. SEM analyses of the tested galvanized samples revealed that the Zn coating had dissolved completely by the end of the immersion tests in 10^{-2} mol dm^{-3} NaCl, indicating a generalized corrosion process. The SEM micrograph of the samples exposed to the tropical marine environment for 14 months (Figure 3b) showed the occurrence of localized dissolution of the layer, which was also observed in samples exposed for 36 months. The localized corrosion of the exposed galvanized steel tested here was congruent with the behavior observed by ref. [15] in Zn electrocoatings also exposed to a marine environment.

Figure 4a shows the as-received galvannealed layer, which displayed cracks from the surface down to the substrate. A comparison of the cross-section in this micrograph with those presented in the literature [12, 16] confirmed the presence of the δ and Γ phases. The thinner Γ phase had a higher Fe content ($FeZn_4$) and was located at the substrate/coating interface. This phase was considered responsible for the lack of adherence between the Zn–Fe coating and the steel during the stamping process. After the Γ phase, the thicker δ phase ($FeZn_7$) with a lower Fe content was found to prevail in the bulk of the coating. This phase is considered the optimum phase for the stamping process [17]. Additionally, our SEM analyses of the

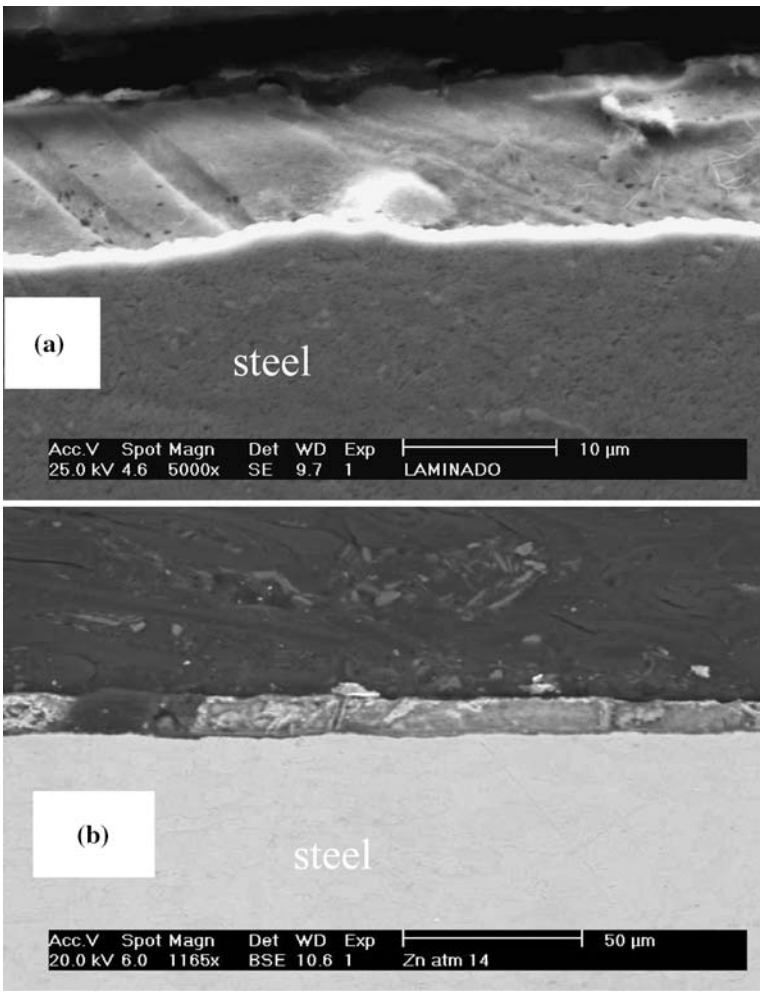

Fig. 3. SEM micrographs showing the cross section of the as-received galvanized steel (a) and as-exposed in a marine atmosphere during 14 months (b).

cross-section indicated that this layer had a homogeneous thickness of 10.5 ± 0.2 µm.

At the end of the immersion tests in aerated 10^{-2} mol dm^{-3} NaCl aqueous solution and after exposure to the natural tropical marine environment, the cross-sections of the galvannealed samples showed a similar morphological evolution toward a more cracked layer (Figure 4b–d). Our SEM analysis revealed cracks distributed throughout the coating. Localized corrosion was also observed in samples exposed for 36 months (Figure 4e). These analyses indicate that the corrosion process in the galvannealed coating was similar in both aqueous solution and marine environment and that it led to and aggravated the occurrence of cracking. The appearance of cracks at the δ/Γ interface, which were absent from the as-received samples, were attributed to galvanic coupling between these phases. These SEM analyses are in close agreement with those of Fabri-Miranda et al. [12], who studied the corrosion of galvannealed steel in an industrial environment over a 1-year period.

Localized EDAX analyses were carried out on the grain and in the cracked region of the tested galvannealed samples after 14 months of exposure to the marine environment, as indicated in Figure 4c. The Fe content in the grain remained about 12.5 at%, while this content in the cracked region was 94.2 at%.

Our GPES, SEM and EDAX analyses showed that the morphological evolution of the cracks was associated with the dissolution of the phases' zinc-rich contents. The literature contains reports of similar results on the evolution of cracking of the Zn–Ni layer during the process of corrosion [14].

3.2. *Corrosion tests*

After 20 days of immersion in 10^{-2} mol dm^{-3} NaCl aqueous solution, the mass loss of the galvannealed and galvanized samples was 124 mg cm^{-2} d^{-1} and 184 mg cm^{-2} d^{-1}, respectively, confirming that, in an aqueous medium, galvannealed steel is more corrosion resistant than galvanized steel.

The potentiodynamic polarization curves of both materials in aerated 10^{-2} mol dm^{-3} NaCl aqueous solution were plotted in order to assess their cathodic and anodic behaviors, which are shown in Figure 5. The corrosion potentials derived from these curves were -1.071 V for galvanized and -0.969 V for galvannealed

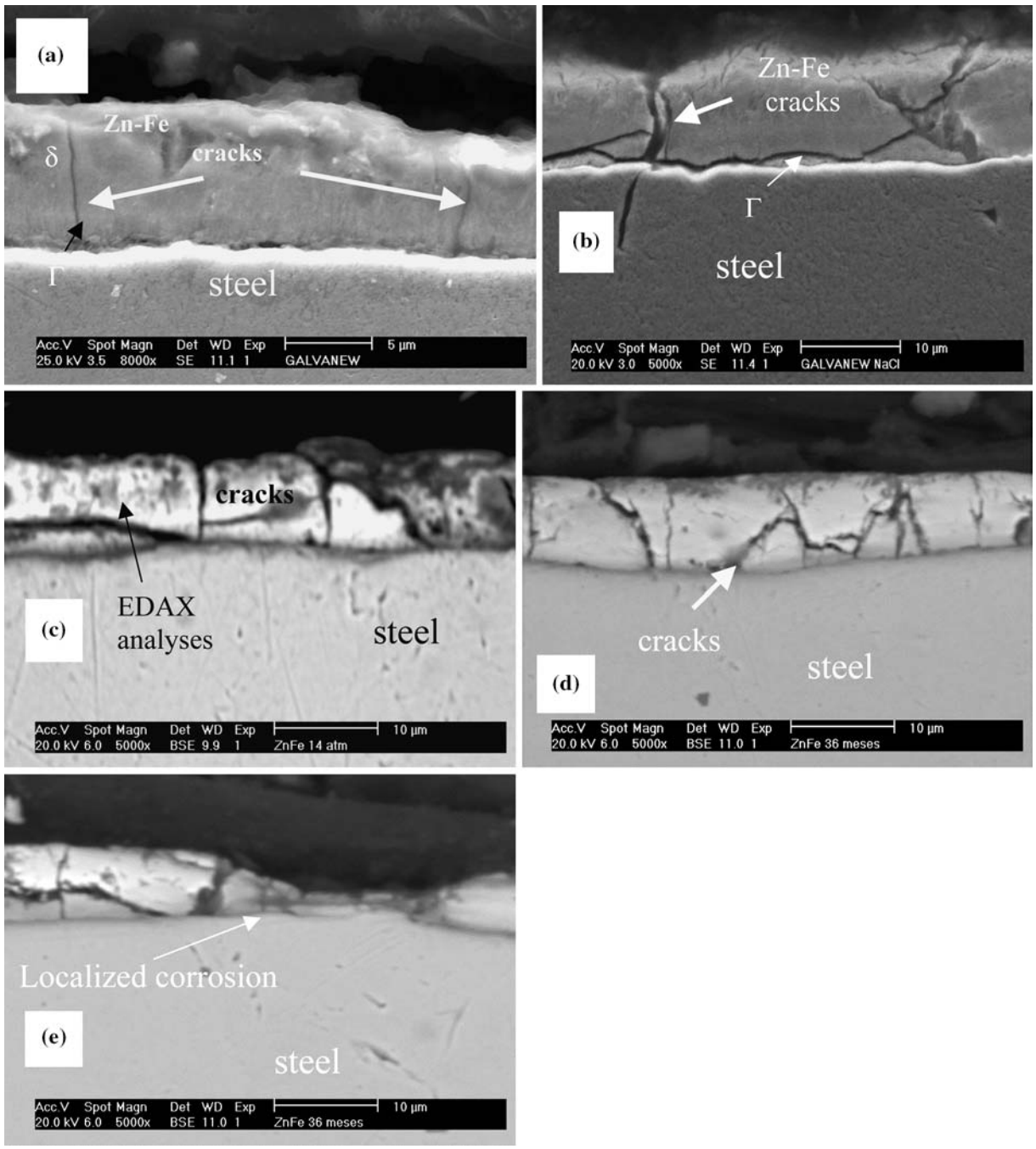

Fig. 4. SEM micrographs showing the cross section of the as-received galvannealed steel (a), as-tested galvannealed steel after the end of immersion tests in 10^{-2} mol dm^{-3} NaCl aqueous solution (b), as-exposed in a marine atmosphere during 14 months (c) and 36 months (d, e).

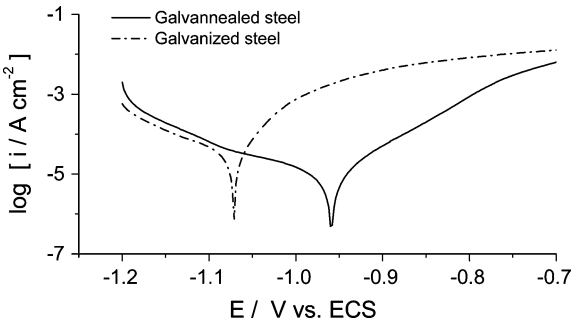

Fig. 5. Potentiodynamic polarization curves obtained for galvannealed steel and galvanized steel in aerated 10^{-2} mol dm^{-3} NaCl aqueous solution at 1 mV s^{-1} and at room temperature.

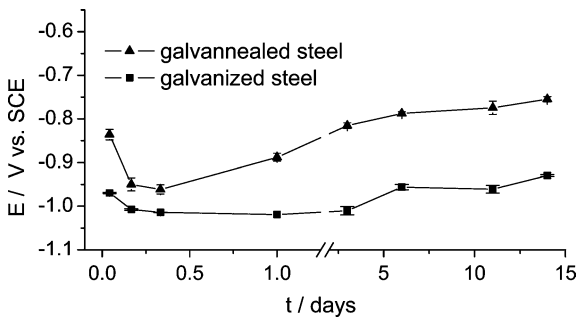

Fig. 6. Evolution of the open circuit potential of the galvannealed (■) and galvanized (▲) samples with time for samples immersed in 10^{-2} mol dm^{-3} NaCl aqueous solution at room temperature.

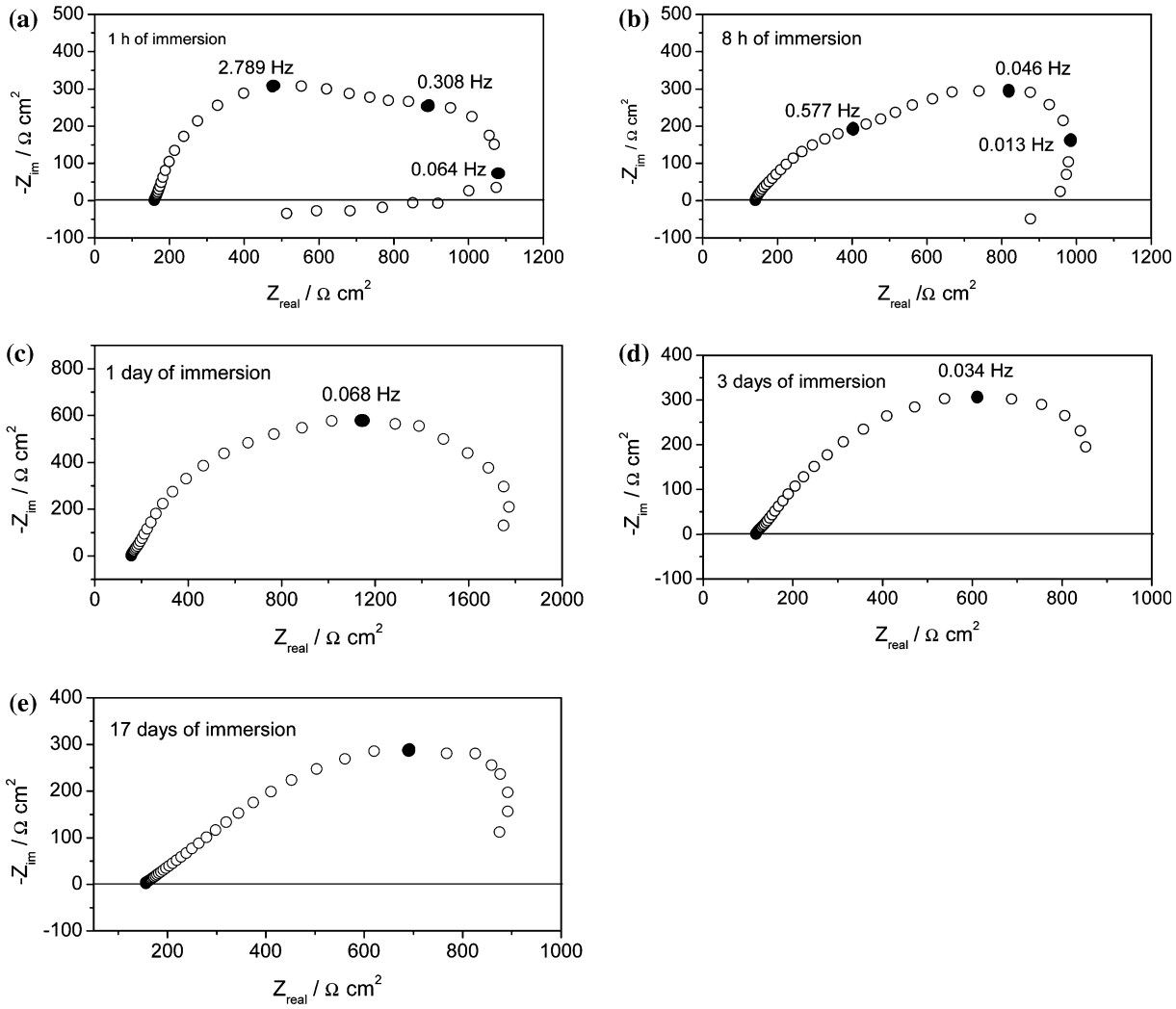

Fig. 7. Evolution of the impedance diagrams with immersion time for galvanized steel samples immersed in 10^{-2} mol dm^{-3} NaCl.

steel, while the polarization resistance indicated by these curves was 0.73 ± 0.08 kΩ cm^{-2} for galvannealed steel and 0.62 ± 0.15 kΩ cm^{-2} for galvanized steel. These results indicate that Zn–Fe coating is nobler and more resistant to generalized corrosion than Zn coating in an aqueous medium.

On the cathodic side, the Tafel slope for the oxygen reduction reaction ($\partial E/\partial \log i$) was about 0.1 V decade^{-1} for both materials, which is highly congruent with that obtained for bare iron [18]. This finding suggests that the cathodic reaction mechanism is the same for both layers. The presence of iron in the galvannealed coating inhibited the cathodic reaction, since the cathodic current densities of galvannealed steel are lower. Additionally, the anodic branch of the polarization curves indicated that these materials showed no passivation in the chloride medium, with the galvannealed steel showing lower anodic current densities than the galvanized steel.

The monitoring E_{oc} is a sensitive measurement to detect the various stages of dissolution of a coating in long-term immersion tests. Figure 6 shows the evolution of the E_{oc} with immersion time for the two materials immersed in aerated 10^{-2} mol dm^{-3} NaCl at room temperature. The end of the process was determined when the surfaces were covered with white corrosion products and isolated red spots.

This figure confirms that the E_{oc} values obtained from the long-term immersion tests are congruous with those obtained in the GES experiments. The E_{oc} corresponding to the galvanized coating remained approximately constant at 1.0 V for 3 days, followed by a gradual increase up the end of the immersion test. The galvannealed coating displayed an initial decrease in the early hours of immersion, followed by a gradual increase until the end of the test. The galvannealed sample presented higher E_{oc} values than the galvanized layer, but lower than the E_{oc} of the steel substrate, indicating that the Zn–Fe coating acted as a sacrificial anode protecting the steel substrate, but that its tendency to corrode was lower than that of the Zn coating. The initial decrease in the E_{oc} of the galvannealed steel is related to the dissolution of the residual Zn in the coating. The increasing E_{oc} with immersion time is explained by the fact that the phases with zinc-rich contents dissolve preferentially, which gradually leads to alloy ennoblement. The dependence of E_{oc} on immersion time

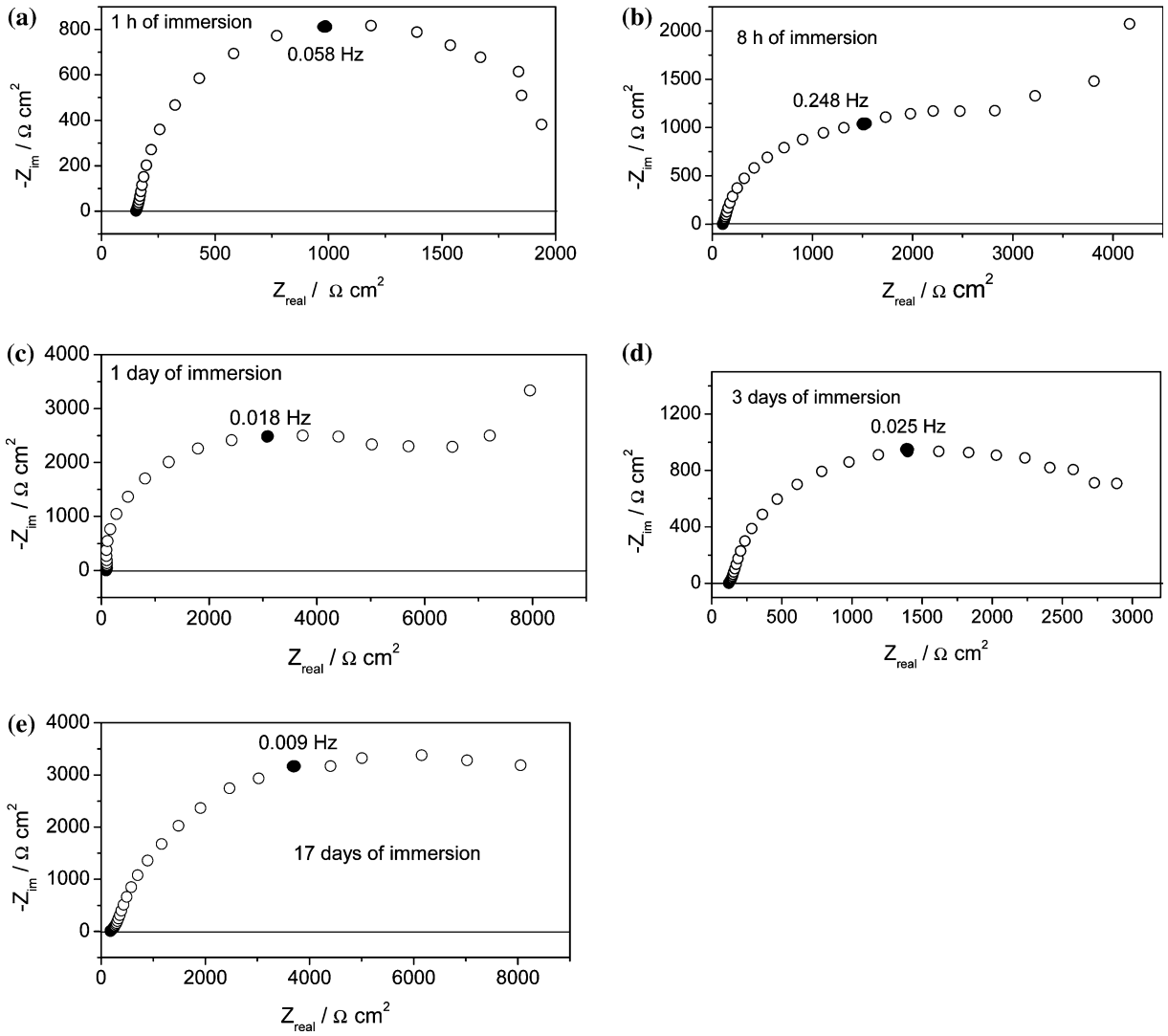

Fig. 8. Evolution of the impedance diagrams with immersion time for galvannealed steel samples immersed in 10^{-2} mol dm^{-3} NaCl.

observed in the Zn–Fe coating is in close agreement with that reported by Baldwin et al. for Zn–Ni electrocoatings [20]. Moreover, Besseyrias et al. [8, 9] pointed out that the similarity between the E_{oc} and GES results for Zn–Fe coating confirms the existence of galvanic coupling between different phases of the coating and that galvanic corrosion is important in this electrolyte, a statement confirmed by our SEM micrographs in Figure 4.

Figure 7 shows the evolution of the impedance diagrams for the galvanized layer as a function of the immersion time in 10^{-2} mol dm^{-3} NaCl aqueous solution; the characteristic frequencies are indicated in each Nyquist plot. The impedance diagrams of the galvanized sample were characterized by three loops in the first 8 h of immersion. The loop in the high frequency range was attributed to the charge transfer resistance (R_{ct}) in parallel with the double layer capacitance (C_{dl}), with measured values ranging from 75 to 100 μF cm^{-2}, which are characteristic of zinc layers [14, 21]. The presence of inductive loops for Zn in an almost neutral solution has been reported previously [22]. With longer immersion times the impedance diagrams evolve to a single capacitive loop.

Figure 8 shows the evolution of the galvannealed steel impedance diagrams as a function of immersion time. After 1 h of immersion, the impedance diagram of the galvannealed sample presents a single capacitive arc relating to the electron transfer reaction at the metal/solution interface, with the measured values of capacitance ranging from 120 to 150 μF cm^{-2}. At immersion times of 4–24 h a diffusion component was observed in the lowest frequency range, probably related to the dissolution of the residual Zn present in the coating. Only a capacitive loop is observed at immersion times of more than 24 h.

Figures 9 and 10 depict the impedance results obtained, for the samples of galvanized and galvannealed steels respectively, tested in the natural marine environment for 36 months. The impedance diagrams for the Zn layer (Figure 9) presented two capacitive loops up to 21 months of exposure time, while the diagram for the sample exposed for 36 months showed three capacitive loops. The impedance diagrams of the

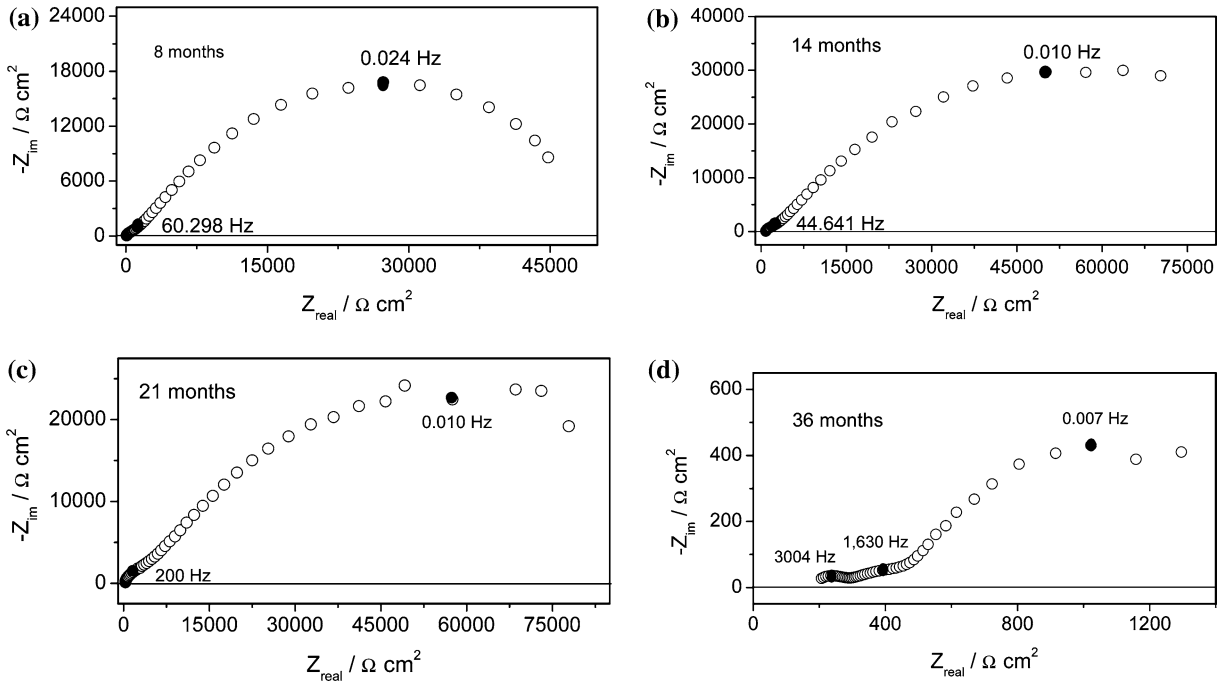

Fig. 9. Evolution of the impedance diagrams with exposing time for galvanized steel samples exposed in tropical marine environment.

Zn–Fe coatings (Figure 10) showed only one capacitive loop except for the one obtained after 21 months.

As Magalhães et al. [23] pointed out, the value of the resistive component of impedance measured at a fixed frequency and in the range of the lower frequencies is very suitable for industrial routines and relates to the corrosion of the coating. Figure 11 shows the values of the real part of the impedance measurement obtained at 10 mHz as a function of immersion time in NaCl solution (Figure 11a) and as a function of exposure time in the natural marine environment (Figure 11b). In the immersion tests the galvannealed steel displayed higher resistance values than the galvanized steel. Additionally, the resistance value of the galvanized steel rose rapidly on the first day of immersion, declining thereafter until the sixth day, when it again showed an upward trend at longer immersion times. On the other hand, the resistance of the galvannealed steel remained approximately constant in the first 8 h of immersion, increasing with longer immersion times. Figure 11b shows that the behavior of the two layers was similar in the natural marine environment, increasing initially up to a

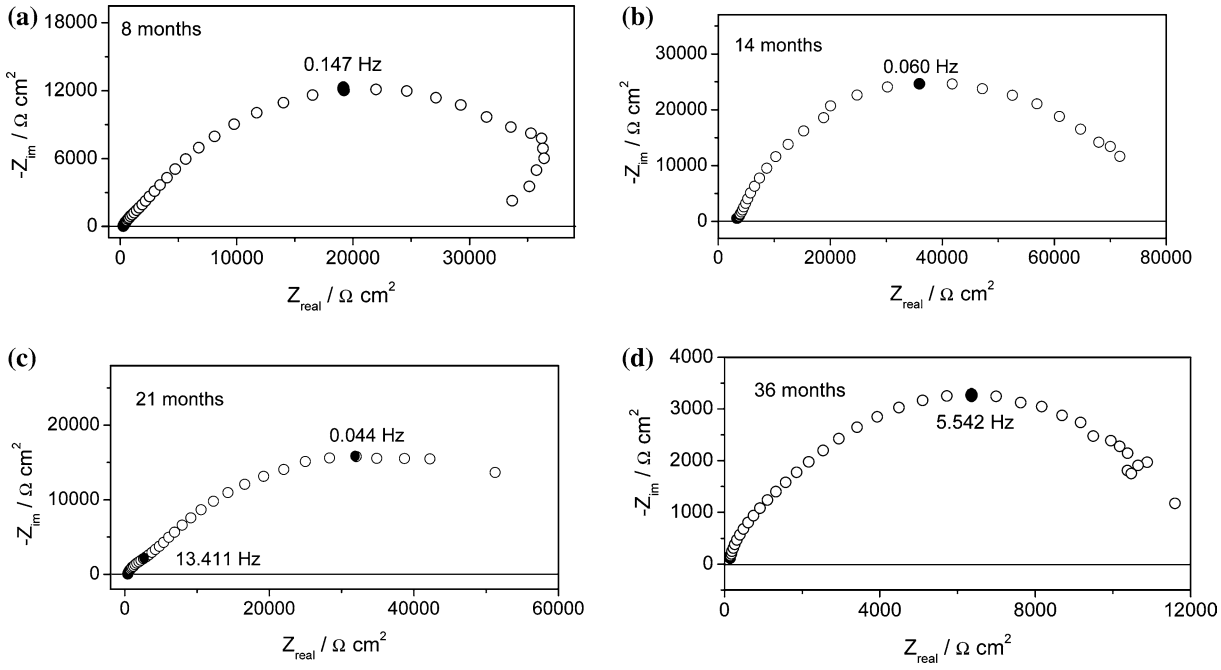

Fig. 10. Evolution of the impedance diagrams with exposing time for galvannealed steel samples exposed in tropical marine environment.

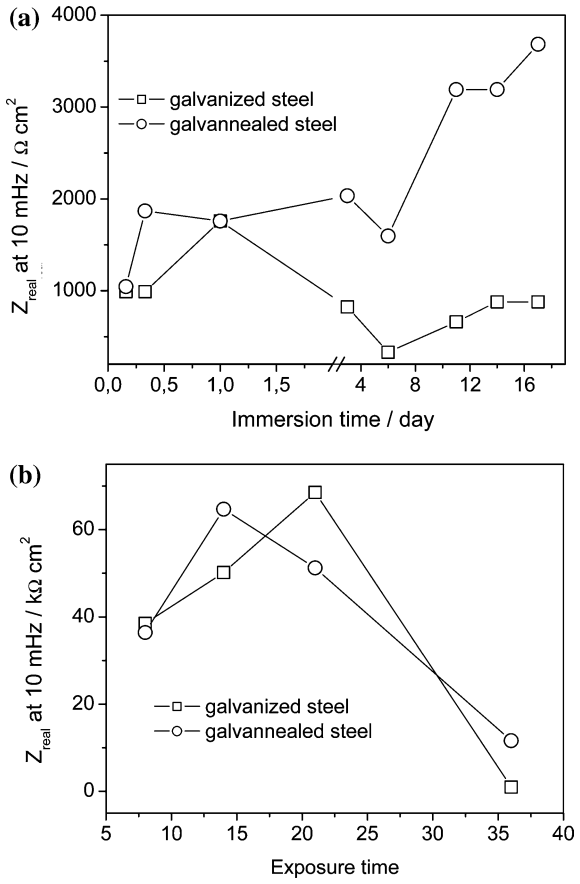

Fig. 11. Z_{real} at 10 mHz vs. immersion time in 10^{-2} mol dm^{-3} NaCl solution (a) and vs. exposure time in tropical marine environment (b).

maximum and then declining gradually until the end of the test.

The increase of the impedance is attributable to the presence of corrosion products on the surface, which improves the barrier properties. However, this improvement in barrier properties does not prevent the localized corrosion process from continuing in both materials (see Figures 3 and 4). In the case of the galvannealed samples, another possible explanation for the increase in total impedance as a function of exposure time is the preferential dissolution of the zinc-rich phases. This assumption is in close agreement with the findings of Lee and Hiam [5], who showed that the dissolution of zinc-rich phases caused the values of polarization resistance to increase.

4. Conclusions

Electrochemical measurements and SEM and EDAX analyses showed the differences in the corrosion behavior of galvanized and galvannealed steel. The corrosion behavior of the galvannealed steel was affected by cracking in the Zn–Fe layer pursuant to the dissolution of zinc-rich phases, while the galvanized steel displayed generalized corrosion in an aqueous medium and localized corrosion in the marine environment. The galvannealed steel showed greater corrosion resistance than the galvanized steel in the aqueous medium. However, the two coatings displayed similar corrosion behavior in the tropical marine environment.

Acknowledgements

The authors thank CNPq-CTPETRO (Proc. 460033/01-8), CAPES and FINEP (Proc. 22.01.0762.00), Brazil, for financial assistance.

References

1. D.T. Llewellyn and R.C. Hudd, *Steels: Metallurgy and Applications*, 3rd ed., (Butterworth Heinemann, Oxford, England, 1998).
2. A.R. Marder, *in* G. Krauss and D.K. Matlock (Eds.), *Zinc-Based Coatings System: Metallurgy and Performance*, (TMS, Warrendale, 1990), p. 55.
3. A.R. Marder, *Prog. Mater. Sci.* **45** (2000) 191.
4. C.R. Shastry and H.E. Towsend, *Corrosion* **45** (1989) 103.
5. H.H. Lee and D. Hiam, *Corrosion* **45** (1989) 852.
6. G. Sergi, N.R. Short and C.L. Page, *Corrosion* **41** (1985) 618.
7. X.G. Chang and I.C. Bravo, *Corrosion* **50** (1994) 308.
8. A. Besseyrias, F. Dalard, J.J. Rameau and H. Baudin, *Corros. Sci.* **37** (1995) 587.
9. A. Besseyrias, P. Giraud, F. Dalard, J.J. Rameau and H. Baudin, *Revue de Métallurgie* **95** (1998) 641.
10. C. Xoffer, H. Dillen and B.C. De Cooman, *J. Appl. Electrochem.* **29** (1999) 209.
11. A. Besseyrias, F. Dalard, J.J. Rameau and H. Baudin, *Corros. Sci.* **39** (1997) 1883.
12. F.J. Fabri Miranda, J.D. da Silva Filho, I.C.P. Margarit and O.R. Mattos, in Proceedings of the 7th International Symposium on Electrochemical Methods in Corrosion Research, paper 95.
13. ASTM G-50 Standard, 03–02, West Conshohocken, PA: ASTM, 183 (1995).
14. F.J. Fabri Miranda, I.C.P. Margarit, O.R. Mattos, O.E. Barcia and R. Wiart, *Corrosion* **55** (1999) 732.
15. A.M. Beccaria, *Corrosion* **46**(11) 906.
16. C.E. Jordan, K.M. Goggins, A.O. Benscoter and A.R. Marder, *Mater. Characterization* **31** (1993) 107.
17. Y. Lin, *Galvatech'98* (ISIJ, Chiba, Japan, 1998), pp. 236.
18. C. Cachet, B. Saidani and R. Wiart, *J. Electrochem. Soc.* **139** (1992) 644.
19. J. O'M Bockris and S.U.H. Khan, *Surface Electrochemistry, A Molecular Leval Approach* (Plenum Press, New York, 1993).
20. K.R. Baldwing, M.J. Robinson and C.J.E. Smith, *Corros. Sci.* **36** (1994) 1115.
21. G. Barceló, M. Sarret, C. Müller and J. Pregonas, *Corros. Sci.* **43** (1998) 13.
22. S. Magaino, M. Soga, K. Sobue, A. Kawaguchi, N. Ishida and H. Imai, *Electrochim. Acta* **44** (1999) 4307 and references cited therein.